Cancer Letters 440–441 (2019) 211–222

Contents lists available at ScienceDirect

Cancer Letters

journal homepage: www.elsevier.com/locate/canlet

Original Articles

HIF-1α-induced miR-23a∼27a∼24 cluster promotes colorectal cancer progression via reprogramming metabolism

Fangfang Jin[a,1], Rong Yang[a,1], Yao Wei[a,1], Dong Wang[a], Yanan Zhu[a], Xiaohua Wang[b], Yousheng Lu[c], Yanbo Wang[a,***], Ke Zen[a,**], Limin Li[a,*]

[a] State Key Laboratory of Pharmaceutical Biotechnology, Jiangsu Engineering Research Center for MicroRNA Biology and Biotechnology, NJU Advanced Institute for Life Sciences (NAILS), School of Life Sciences, Nanjing University, 163 Xianlin Road, Nanjing, Jiangsu, 210046, China
[b] Department of Chemotherapy, Jiangsu Cancer Hospital and Research Institute, Nanjing, Jiangsu, 210009, China
[c] Department of General Surgery, Jiangsu Cancer Hospital and Research Institute, Nanjing, Jiangsu, 210009, China

ARTICLE INFO

Keywords:
miRNA
Feedback
Metabolism reprogramming

ABSTRACT

Tumor cells switch metabolic profile from oxidative phosphorylation to glycolysis in a hypoxic environment for survival and proliferation. The mechanisms governing this metabolic switch, however, remain incompletely understood. Here, we show that three miRNAs in the miR-23a∼27a∼24 cluster, miR-23a, miR-27a and miR-24, are the most upregulated miRNA cluster in colorectal cancer (CRC) under hypoxia. Gain- and loss-of-function assays, a human glucose metabolism array and gene pathway analyses confirm that HIF-1α-induced miR-23a∼27a∼24 cluster collectively regulate glucose metabolic network through regulating various metabolic pathways and targeting multiple tricarboxylic acid cycle (TCA)-related genes. In specific, miR-24/VHL/HIF-1α in CRC form a double-negative feedback loop, which in turn, promotes the cellular transition to the 'high HIF-1α/miR-24 and low VHL' state and facilitates cell survival. Our findings reveal that the miR-23a∼27a∼24 cluster is critical regulator switching CRC metabolism from oxidative phosphorylation to glycolysis, and controlling their expression can suppress colorectal cancer progression.

1. Introduction

Hypoxia is a hallmark of solid tumors and represents a key regulatory factor in tumor growth and survival [1,2]. Tumor cells modify their energy sources to adapt to challenging hypoxic environments and synthesize macromolecules at sufficient rates to meet the demands of malignant proliferation [2,3]. For example, tumor cells coordinate metabolic activities to produce ATP. A common characteristic of cancer cells is their reprogramming of cellular metabolism to favor metabolic pathways that fuel aberrant cell growth and proliferation [4,5]. Constitutive upregulation of glycolysis can also provide a survival advantage for tumor cells because limitations in tumor vascularization result in periods of intermittent hypoxia that require a cancer cell, such as the CRC cell [6], to rely on glycolysis [7]. Therefore, hypoxia represents an important selection pressure that drives the clonal progression of tumors, linking metabolic dysregulation to tumor progression.

MicroRNAs (miRNAs) regulate gene expression at the post-transcriptional level by binding to the 3′-untranslated regions (UTRs) of target mRNAs to either block mRNA translation or trigger mRNA degradation [8]. MiRNAs regulate diverse cellular functions and play important roles in various physiological and pathological cellular processes, including metabolic reprogramming [9]. Individual miRNAs are involved in regulating the glycolytic switch in cancer cells [10,11], however, at times, the effect of an individual miRNA is insufficient to drive such metabolic changes. In contrast, cluster miRNAs, which are organized in the genome within 3 kb and transcribed coordinately as polycistronic units, can trigger substantial biological consequences [12,13]. Therefore, this property can be used to link miRNA clusters to the regulatory networks that govern cancer metabolic reprogramming.

The coordinated homeostatic response to hypoxia is largely transcriptional and mediated mainly through the activation of the heterodimeric transcription factor hypoxia-inducible factor (HIF)-1 [2]. HIF-1, which is a heterodimer that comprises HIF1-α and HIF1-β, is a key

* Corresponding author.
** Corresponding author.
*** Corresponding author.
E-mail addresses: ybwang@nju.edu.cn (Y. Wang), kzen@nju.edu.cn (K. Zen), liminli@nju.edu.cn (L. Li).
[1] These authors contributed equally to this work.

https://doi.org/10.1016/j.canlet.2018.10.025
Received 29 June 2018; Received in revised form 1 October 2018; Accepted 16 October 2018

regulator of the transcriptional response to hypoxia. Under normoxia, HIF1-α is hydroxylated at key proline residues, which facilitates von Hippel–Lindau tumor suppressor (VHL) protein binding with consequent ubiquitination and subsequent proteasome-targeted degradation [14]. Under hypoxic conditions, proline hydroxylation is inhibited, which allows HIF1-α to escape VHL recognition and become stabilized. HIF1-α can then translocate to the nucleus and bind to constitutively expressed HIF1-β to form the active HIF-1 complex. The HIF-1 complex recruits p300/CBP, a transcriptional activator, which enhances transcriptional activity [15]. The HIF-1 transcriptional response largely allows cellular adaptation to the hypoxic microenvironment and regulates metabolic reprogramming, which serves to increase glucose uptake, glycolysis, angiogenesis and stress resistance [16,17]. HIF-1α is overexpressed in several types of cancer, including CRC, and compelling evidence supports a role for HIF-1α in tumorigenesis [18]. However, the underlying mechanism for the continuous upregulation of HIF-1α in tumors remains to be elucidated.

To investigate the functions and involvement of miRNAs in metabolic reprogramming and tumorigenesis, we screened significantly dysregulated miRNAs under hypoxia. We identified a miRNA cluster, namely, the miR-23a∼27a∼24 cluster, to be markedly upregulated under hypoxia. HIF-1α could bind to the promoter region of the miR-23a∼27a∼24 cluster and induce miR-23a∼27a∼24 cluster expression in CRC cells. Our *in vitro*, *in vivo* experiments and clinical patient samples highlighted the important role of the miR-23a∼27a∼24 cluster toward linking hypoxia to glycolysis. A human glucose metabolism array revealed that miR-23a∼27a∼24 cluster extensively regulate cancer metabolic networks and further shifted the balance toward glycolysis. Mechanistically, miR-24/VHL/HIF-1α formed a double-negative feedback loop, which could amplify the effect of HIF-1α and miR-23a∼27a∼24 cluster. Collectively, our findings reveal the miR-23a∼27a∼24 cluster as a robust modulator of glycolysis and a promising therapeutic target for CRC treatment, and also adds a new dimension to hypoxia-mediated regulation of colorectal cancer metabolism.

2. Materials and methods

2.1. Cell lines

HT-29, Caco2 and SW480 were obtained from Shanghai Institute of Cell Biology, Chinese Academy of Sciences (Shanghai, China). HT-29, SW480 and Caco2 cells were cultured in RPMI-1640 (GIBCO, Carlsbad, CA, USA) and DMEM (GIBCO), respectively. The media were supplemented with 10% fetal bovine serum (GIBCO) and 1% penicillin–streptomycin, and cells were cultivated in 5% CO_2 at 37 °C in a humidified atmosphere. For hypoxia culture, cells were transferred to a hypoxia chamber with 1% oxygen. The cells used for functional and mechanism experiments were tested and authenticated using the short tandem repeat (STR) method by Shanghai Institute of Cell Biology.

2.2. RNA isolation and Small-RNA sequencing

Total RNA was purified with a Trizol Reagent Kit (Life Technologies) and treated with DNase I to remove trace amounts of DNA contamination. Small-RNA Sequencing and data analysis were entrusted to Novogene (Beijing, China) as previously described [19]. The small RNA sequence data have been uploaded to NCBI Sequence Read Archive (SRA) (Accession Number: PRJNA493892).

2.3. miRNA-related reagents, siRNA, and transfection

The miRNA mimics, inhibitors, negative controls, VHL siRNA (target sequence: CCGTATGGCTCAACTTCGA) and HIF-1α siRNA (target sequence: GAAGGAACCTGATGCTTTA) were purchased from RIBOBIO (Guangzhou, China). For the VHL and HIF-1α overexpression assays, the pcDNA3.1 vectors that were designed to specifically express the open reading frames (ORFs) of human VHL and HIF-1α with the full-length 3′-UTRs were purchased from GenScript (Nanjing, China). The transfections were performed as we described previously [20].

2.4. Rreal-time quantitative PCR

Total RNA extraction, reverse transcription and Real-time PCR were performed as we described previously [20]. The sequences of primers used are shown in Supplementary Table 1. For the analysis of glucose metabolism-associated gene expression, cDNA was synthesized using the RT^2 First Strand Kit (Qiagen, Germany) and samples were analyzed for expression of 84 genes that are involved in regulation of glucose metabolism using the RT^2 Profiler PCR Human Glucose Metabolism Array (PAHS-006Z, Qiagen) as described previously [10,21].

2.5. Western blotting

Cellular protein was extracted as described previously [12]. Antibodies against VHL(sc-17780, Santa Cruz Biotechnology, CA, USA), PKM2(#4053, Cell Signaling Technology, CA, USA), Histone H2A (#7631, Cell Signaling Technology, CA, USA), HIF-1α (ab1, Abcam, UK), ACLY (ab40793), ACO1 (ab126595), CS (ab96600), DLD (sc-365977, Santa Cruz Biotechnology, CA, USA), IDH1 (ab172964), IDH2 (ab131263), IDH3A (ab58641), MDH1B (ab173722), PCK1 (ab133603), PDHA1 (ab168379), PDHB (ab155996), SDHA (ab137040), SDHD (ab189945, Abcam, UK) and β-actin (#4970, Cell Signaling Technology, CA, USA) were used for blotting. β-actin served as internal control. All band intensity was quantified using ImageJ v1.50e (NIH, Bethesda, Maryland) and normalized to internal control.

2.6. Nucleus extraction

The nuclear fraction of cells was extracted using a PARIS™ kit (Ambion, AM1921) as we described previously [22].

2.7. Luciferase assay

For the luciferase reporter assay, the p-MIR-REPORT plasmids were purchased from GenScript (Nanjing, China) and designed to contain the 3′-UTRs of human ACO1, CS, PDHB, IDH1, SDHD, PDHA1, IDH2, DLD, ACLY, IDH3A, MDH1B, PCK1, SDHA and VHL. The 293T cells were co-transfected with the β-galactosidase (β-gal) expression plasmid (as transfection control normalization) (Ambion, USA), a firefly luciferase reporter plasmid, and miR-23, miR-24, miR-27 mimics or a negative control. The β-gal plasmid was used as a transfection control. Luciferase activity was measured 24 h after transfection using a luciferase assay kit (Promega, Madison, WI, USA). Additionally, to test the direct binding of HIF-1α to the promoter of the miR-23a∼27a∼24 cluster, a synthetic 300-bp DNA fragment (GenScript), which included the binding sequence in the miR-23a∼27a∼24 promoter region, was inserted into the promoter region of the pGL3 basic plasmid (Ambion), and the insertion was confirmed by sequencing. To test the binding specificity, the sequences that interacted with HIF-1α were mutated, and the mutated DNA fragments were also inserted into the promoter region of the pGL3 basic plasmid. The 293T cells were cultured in 24-well plates, and each well was transfected with 0.1 μg firefly luciferase reporter plasmid, 0.1 μg β-gal expression plasmid (Ambion) and 0.1 μg HIF-1α overexpression plasmid or negative control plasmid using Lipofectamine 2000 (Invitrogen). The β-gal plasmid was used as a transfection control. Twenty-four hours after transfection, the cells were examined using a luciferase assay kit (Promega, Madison, WI, USA) [20].

2.8. Chromatin immunoprecipitation (ChIP)

ChIP assays were carried out using an EZ-ChIP assay kit (Millipore, Massachusetts, USA) in accordance with the manufacturer's instructions [12]. Soluble chromatin was prepared from HT-29 cells and incubated with an anti-HIF-1α antibody (Abcam, UK) or human IgG (negative control). The primer pairs used for the PCR analysis were as follows: for site 1, 5′-TGGTGGCTCACGCCTGTA-3' (forward) and 5′-CCCGAGTAG CTGGGATTA-3' (reverse) and for site 2, 5′-GGCTGGTCTTGAACTCCT-3' (forward) and 5′-CCTTGCTCCACAGTTTCC-3' (reverse). All data were normalized to the input.

2.9. Measurement of lactate production and glucose uptake and ATP production

Extracellular lactate was measured in the cell culture medium using a lactate assay kit (BioVision, #K607-100) and intracellular glucose was measured in the cell lysates using a glucose assay kit (BioVision, #K606-100) as described previously [23] [10]. The cellular ATP levels in CRC cells were determined with a CellTiter-Glo Assay kit (Promega) and luminometer (Promega) according to the manufacturer's protocols. The relative ATP levels (measured as luminescence) were normalized to the respective cell lysate protein concentration.

2.10. Measurement of ROS production

CRC cells and tumor slices were harvested, washed and incubated with 5 μmol/l dichlorofluorescein diacetate (DCFH-DA, Beyotime) at 37 °C for 30 min in the dark. Cells and tumor slices were then harvested, washed and resuspended in serum-free culture medium. The DCF fluorescence distribution was recorded (DCF: the excitation wavelength was 488 nm, and the emission wavelength was 525 nm).

2.11. In situ hybridization

In situ hybridization of human CRC tissues was performed using a miRCURY LNA™ microRNA probe (Exiqon, Denmark) that was directed against hsa-miR-24-3p (probe Sequence: TGTTCCTGCTGAACTGAG CCA), hsa-miR-23a-3p (probe Sequence: AAATCCCTGGCAATGTGA) and hsa-miR-27a-3p (probe Sequence: CGGAACTTAGCCACTGTGAA). To detect the *in situ* expression of hsa-miR-24-3p, hsa-miR-23a-3p and hsa-miR-27a-3p, the procedure was performed as described previously [20].

2.12. Immunofluorescence and immunohistochemistry

Immunofluorescence staining was performed as described previously [20,24]. To evaluate tumor histological changes, tumor sections were processed for H&E staining as described [20]. Immunohistochemical staining of the paraffin sections was performed using a microwave-based antigen retrieval technique, and specimen slides were incubated overnight at 4 °C with primary antibodies that were raised against Ki-67 (Cell Signaling Technology, USA), HIF-1α (Abcam, UK) and VHL (Santa Cruz Biotechnology, CA, USA). Immunofluorescence and immunohistochemistry were quantitated using Image-Pro Plus 6.0 software.

2.13. Animal studies

The 6-week-old male SCID mice (nu/nu) were obtained from the Model Animal Research Center of Nanjing University (Nanjing, China). All animal studies were conducted with approval from the Animal Research Ethics Committee of Nanjing University. For xenograft experiments, CRC cells were infected with miR-23a/27a/24-overexpressing lentiviral vector or anti-miR-23a/27a/24 lentiviral vector or transfected with the VHL expression plasmids. Lentiviral vector was purchased from GenePharma (Shanghai, China) and constructed according to the methods described previously [25–27]. The cells were injected subcutaneously into SCID mice (1×10^6 cells per mouse, 6 mice per group). The mice were sacrificed 24 days later, and tumors were resected. The length, width and height of each tumor was measured using digital calipers, and the ellipsoid volume was calculated using the following formula: Volume = $\pi/6 \times$ (length) $\times$ (width) $\times$ (height). The tumor tissues were fixed for further H&E staining and immunohistochemistry assays. To measure the metabolic state of the tumor, each tumor was finely minced, ground, and digested with RPMI-1640 containing 1 mg/ml collagenase D and 100 U/ml DNase I for 45 min at 37 °C and passed through a 70-mm nylon cell strainer, centrifuged to remove the large pieces of tissue, and depleted of red blood cells. Tumor-cell suspensions were generated and cultured to determine the metabolic parameters.

2.14. Clinical human CRC specimens

36 paired CRC and normal adjacent tissues were obtained from consenting patients, and the experiments were approved by Jiangsu Cancer Hospital and Research Institute. The clinical features of the patients are listed in Supplementary Table 2.

2.15. TCGA (The cancer genome Atlas) database

The miRNA and mRNA sequencing data, along with clinical information, were obtained from TCGA data portal (https://xenabrowser.net/datapages/?cohort=TCGA%20Colon%20Cancer%20(COAD)) [28].

2.16. Statistical analysis

The data are presented as the mean ± SEM of at least three independent experiments. Differences between groups were analyzed using Student's *t*-test. Differences between more than two groups were analyzed using ANOVA. Throughout the text, figures, and figure legends, the following terminology is used to denote statistical significance: *P < 0.05, **P < 0.01, and ***P < 0.001.

3. Results

3.1. Hypoxia stimulates the expression of miR-23a~27a~24 cluster in CRC

To investigate the regulatory roles of miRNAs in CRC under hypoxia, HT-29 cells were grown in hypoxia (1% O_2, 48 h) or normoxia. The raw data of distinct miRNA expression profiles were submitted to the online public database (SRA accession: PRJNA493892). The supervised hierarchical cluster analysis were performed to determine the miRNA profiles under hypoxia (Fig. 1a). Intriguingly, hypoxia led to a common upregulation of miRNAs in CRC cells, including miR-210, miR-27a, miR-182, miR-142, miR-101, miR-23a, miR-24 and so on. Interestingly, among the most upregulated miRNAs, 3 miRNAs (miR-23a, miR-27a and miR-24) belonged to the miR-23a~27a~24 cluster (Fig. 1a). The increased miRNAs were then validated by quantitative RT-PCR (qRT-PCR) in HT29, SW480 and Caco2 cell lines (Fig. 1b), suggesting that miR-23a~27a~24 cluster is a potentially important regulatory group of miRNAs involved in hypoxia-induced cellular responses. Tumor tissues from CRC patients were classified hypoxic tissues, based on the staining of HIF-1α and carbonic anhydrase-9 (CA9), an endogenous hypoxic marker (Fig. 1c). Likewise, miR-23a~27a~24 cluster was observed to be significantly upregulated in 36 pairs of human CRC tumors compared to matched normal adjacent tissues by qRT-PCR and *in situ* hybridization assays (Fig. 1d, Supplementary Fig. 1). The finding was further explored upon interrogation of TCGA datasets, which revealed that the expression of miR-23a~27a~24 cluster was significantly increased in CRC tumor tissue compared to

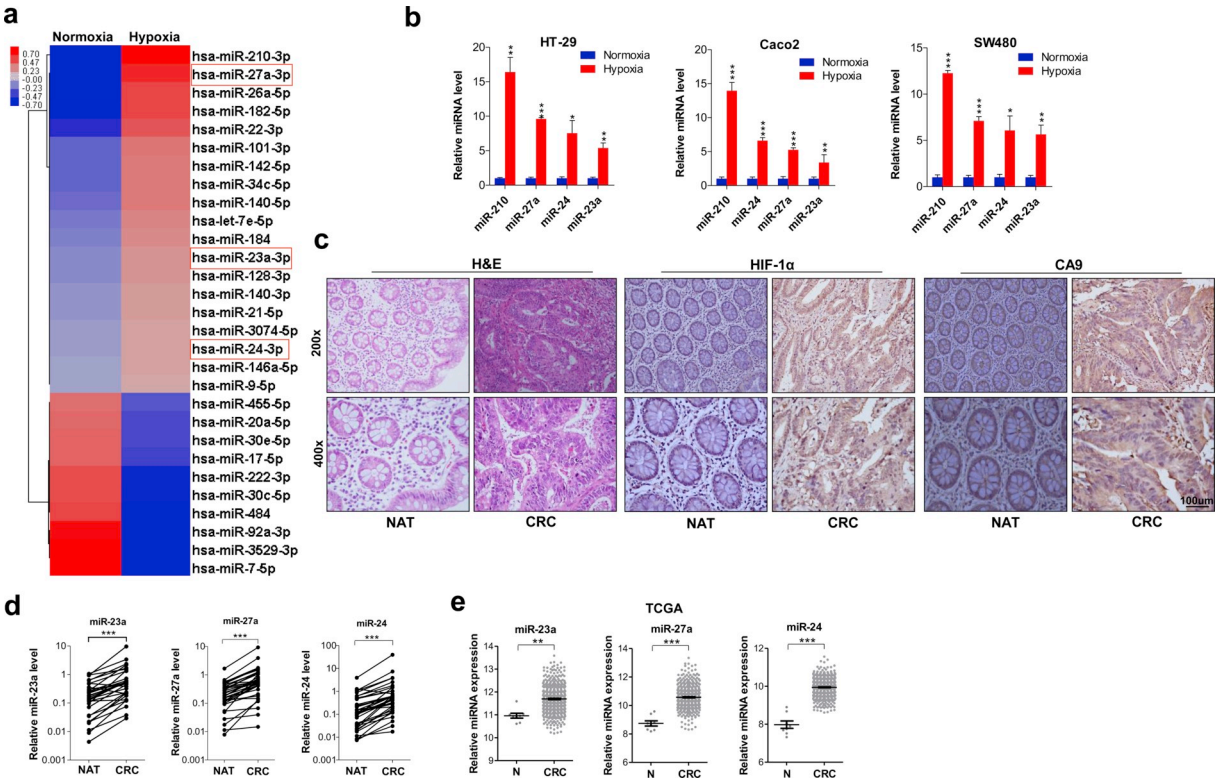

Fig. 1. Distinct expression of miR-23a ~ 27a ~ 24 cluster under hypoxia. (a) The effect of hypoxia on expression of miRNAs in HT-29 cell line. The heatmap represents differentially expressed miRNAs at 48 h after culturing under hypoxia with the upregulated miRNAs in red and downregulated miRNAs in blue. **(b)** The relative miRNA levels in HT-29, Caco2 and SW480 cells after culturing under hypoxia were verified by qRT-PCR. **(c)** Representative histological section figures, immunohistochemical staining of HIF-1α and CA9, an endogenous hypoxic marker, in CRC tumor tissues and normal adjacent tissues. **(d)** The relative levels of miR-23a, miR-24 and miR-27a in tumor tissues (CRC) and normal adjacent tissues (NAT) were determined by qRT-PCR, n = 36 in each group. **(e)** Scatter plots showing relative expression levels of miR-23a ~ 27a ~ 24 cluster members in non-tumor (N), and CRC cancer tissues (CRC) from TCGA patients. Data are shown as the mean ± S.E. of three separate experiments. *P < 0.05, **P < 0.01, ***P < 0.001. (For interpretation of the references to color in this figure legend, the reader is referred to the Web version of this article.)

normal tissue (Fig. 1e).

3.2. HIF-1α stimulates the expression of miR-23a ~ 27a ~ 24 cluster via the specific HIF-1α binding motifs

We next explored how hypoxia increase the miR-23a ~ 27a ~ 24 cluster expression in CRC cells. Immunoblot analysis confirmed that HIF-1α was significantly induced by hypoxia in HT-29 cells (Fig. 2a). To explore the correlation between HIF-1α and miR-23a ~ 27a ~ 24 cluster, we overexpressed and knocked down HIF-1α in HT-29 cells and measured the response of miR-23a ~ 27a ~ 24-2 cluster by qRT-PCR. Efficient knockdown and overexpression of HIF-1α in HT-29 cells were shown in Supplementary Fig. 2. Ectopic expression of HIF-1α resulted in an increase in miR-23a ~ 27a ~ 24 expression (Fig. 2b), whereas knockdown of HIF-1α using siRNA resulted in a decrease in miR-23a ~ 27a ~ 24 expression (Fig. 2c). Similar alterations of the precursors levels of miR-23a ~ 27a ~ 24-2 cluster were observed (Fig. 2d and e). In TCGA CRC patient datasets, the expression level of miR-23a ~ 27a ~ 24 significantly and positively correlated with that of HIF-1α (Fig. 2f). These results suggest that the alterations to miR-23a ~ 27a ~ 24 cluster were likely due to transcriptional changes.

HIF-1α binds to the promoters of target genes through motifs that consist of a 5′-GACGTGACTT-3′ sequence to activate gene transcription [29,30]. Using this motif, we predicted putative HIF-1α binding sites in the promoter region of miR-23a ~ 27a ~ 24 cluster. Interestingly, the genomic analysis identified two putative HIF-responsive elements (HREs) within the promoter region of miR-23a ~ 27a ~ 24-2 cluster (Fig. 2g). To addressed whether HIF-1α directly bind to these HREs, we performed chromatin immunoprecipitation (ChIP) assays in HT-29 cells. The results confirmed that HIF-1α was recruited to binding site 2 (HRE2) in miR-23a ~ 27a ~ 24-2 promoter (Fig. 2h and i). Next, we cloned the HRE2 sequence into upstream region of a firefly luciferase reporter gene and transfected the resulting plasmids into 293T cells. Luciferase reporter assays revealed that ectopic expression of HIF-1α promoted transcription of firefly luciferase in plasmids with the HRE2 sequence inserted into promoter region. However, when the HRE2 sequence was mutated, the firefly luciferase activity was unaffected by HIF-1α overexpression (Fig. 2g and j). Taken together, these results demonstrate that HIF-1α promotes the transcription of miR-23a ~ 27a ~ 24-2 cluster via specific binding motif in promoter region.

3.3. Potential roles of miR-23a ~ 27a ~ 24 cluster in glucose metabolism

Then we conducted bioinformatics analysis to identify the potential functions that underlie the enhanced expression of miR-23a ~ 27a ~ 24 cluster. Target genes of three miRNAs were predicted using TargetScan, miRbase and Miranda, and a microarray-based Gene Ontology (GO) analysis was performed to identify biological processes that might be associated with these target genes [31,32]. Of the GO functional categories for miR-23a, metabolism-related genes accounted for 50%. Likewise, among the high-enrichment GOs targeted by miR-24 and miR-27a, 47.7% and 38.6% genes were involved in metabolism-related processes, respectively (Supplementary Fig. 3A). The results suggest that miR-23a ~ 27a ~ 24 cluster may be involved in regulating metabolism-related processes in cells.

These target genes were further analyzed by functional enrichment based on KEGG (Kyoto Encyclopedia of Genes and Genomes) pathways via DAVID (The Database for Annotation, Visualization and Integrated

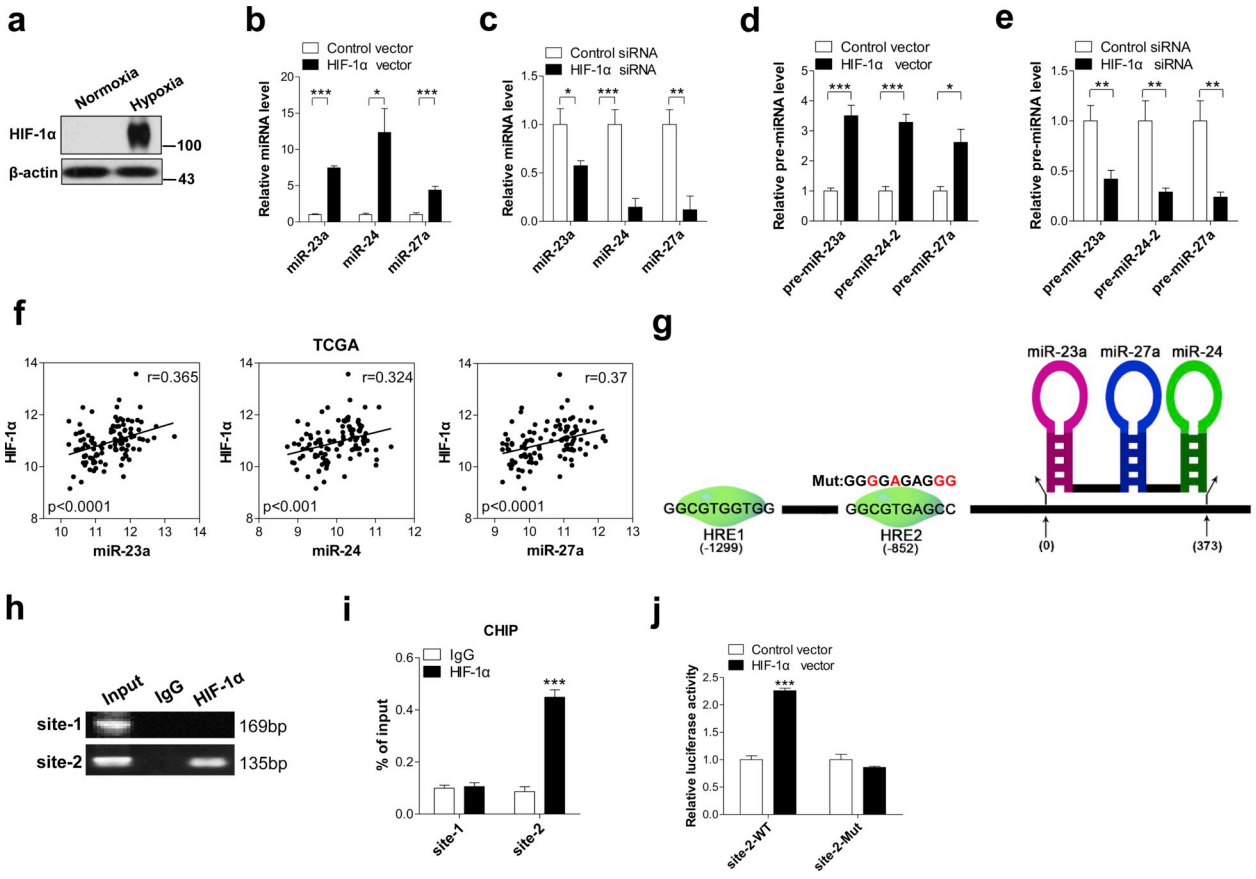

Fig. 2. HIF-1α directly induces the expression of miR-23a∼27a∼24 cluster by binding to the regulatory motif of miR-23a∼27a∼24 promoter. (a) Representative western blot analyses of HIF-1α in HT-29 cells under hypoxia for 48 h, β-actin was served as internal control. **(b, d)** qRT-PCR analysis showing that HIF-1α overexpression upregulates the expression of miR-23a, miR-24, miR-27a, pre-miR-23a, pre-miR-24 and pre-miR-27a in HT-29 cells. **(c, e)** qRT-PCR analysis showing that HIF-1α knockdown by siRNA downregulates the levels of miR-23a, miR-24, miR-27a, pre-miR-23a, pre-miR-24 and pre-miR-27a in HT-29 cells. **(f)** Pearson's correlation scatter plot of miR-23a∼27a∼24 cluster and HIF-1α in TCGA CRC patients. **(g)** A schematic diagram of two putative HIF-1α-binding motifs (HRE1 and HRE2) in miR-23a∼27a∼24-2 promoter. **(h)** Robust PCR product enrichment that indicates HIF-1α binding is shown in the HIF-1α lane. Negative control amplification was carried out using rabbit IgG-immunoprecipitated chromatin (IgG lane). Positive control amplification was carried out using input chromatin before immunoprecipitation (Input lane). Binding of HIF-1α to site 2, but not to site 1, was confirmed by semi-quantitative PCR followed by gel electrophoresis and quantitative PCR **(i)** using primers that were specific for the two sites. **(j)** Luciferase reporter assays confirming the direct binding of HIF-1α to miR-23a∼27a∼24-2 promoter through binding motif 2 (site 2). Data are shown as the mean ± S.E. of three separate experiments. *P < 0.05, **P < 0.01, ***P < 0.001.

Discovery) [31,33], ten pathways were enriched with statistical significance. High numbers of significantly regulated genes were evident among the glucose metabolic pathway genes that are associated with TCA, glycosphingolipid biosynthesis, proteoglycans in cancer, the AMPK signaling pathway, the PI3K-Akt signaling pathway and the insulin signaling pathway (Supplementary Fig. 3B), these pathways synergistically maintain energy and redox homeostasis in cellular metabolism [16,34]. Taken together, these results suggest the potential involvement of miR-23a∼27a∼24 cluster in glucose metabolism via signaling pathways.

3.4. The miR-23a∼27a∼24 cluster promotes CRC glycolysis in vitro and in vivo

We further verified whether miR-23a∼27a∼24 cluster regulates cancer metabolism *in vitro* and *in vivo*. HT-29 and Caco2 cells were transfected with miR-NC, miR-23a/27a/24 mimics (a combination of miR-23a mimic, miR-24 mimic and miR-27a mimic), anti-miR-NC and anti-miR-23a/27a/24 (a combination of an anti-miR-23a inhibitor, anti-miR-24 inhibitor and anti-miR-27a inhibitor) under hypoxia, normoxic cells served as controls. The measurements of metabolic parameters revealed that the cellular glucose uptake and lactate levels in the medium were increased significantly in CRC cells that were transfected with miR-23a/27a/24 mimics in hypoxic state (Fig. 3a and b), whereas miR-23a/27a/24 knockdown markedly decreased the glucose uptake and lactate production of CRC cells (Fig. 3a and b). Because ATP and ROS are important indicators of tumor survival, growth, and expansion [35–37], we measured cellular ATP and ROS levels under hypoxia and observed that miR-23a/27a/24 overexpression led to increased cellular ATP and ROS levels (Fig. 3c and d, Supplementary Fig. 4A). Conversely, cellular ATP production and ROS levels were markedly decreased in cells transfected with anti-miR-23a/27a/24 (Fig. 3c and d, Supplementary Fig. 4A). We also measured two important HIF-1α target genes critical for increased glucose uptake and catabolism via glycolysis: glucose transporter 1 (GLUT1) and hexokinase II (HK2) [38,39]. miR-23a/27a/24 overexpression increased GLUT1 and HK2 expression significantly, whereas miR-23a/27a/24 knockdown resulted in reduced GLUT1 and HK2 expression in CRC cells (Fig. 3 e and f). Collectively, these data indicate that miR-23a∼27a∼24 cluster promotes glycolysis in CRC cells.

To further explore the role of miR-23a∼27a∼24 cluster in tumor growth and metabolism, HT-29 cells were infected with miR-23a/27a/24 lentiviral vectors to co-express miR-23a, miR-24 and miR-27a or infected with anti-miR-23a/27a/24 lentiviral vectors to block the expression of miR-23a, miR-24 and miR-27a. The infected cells (1×10^6 cells per 0.1 ml) were implanted subcutaneously into nude

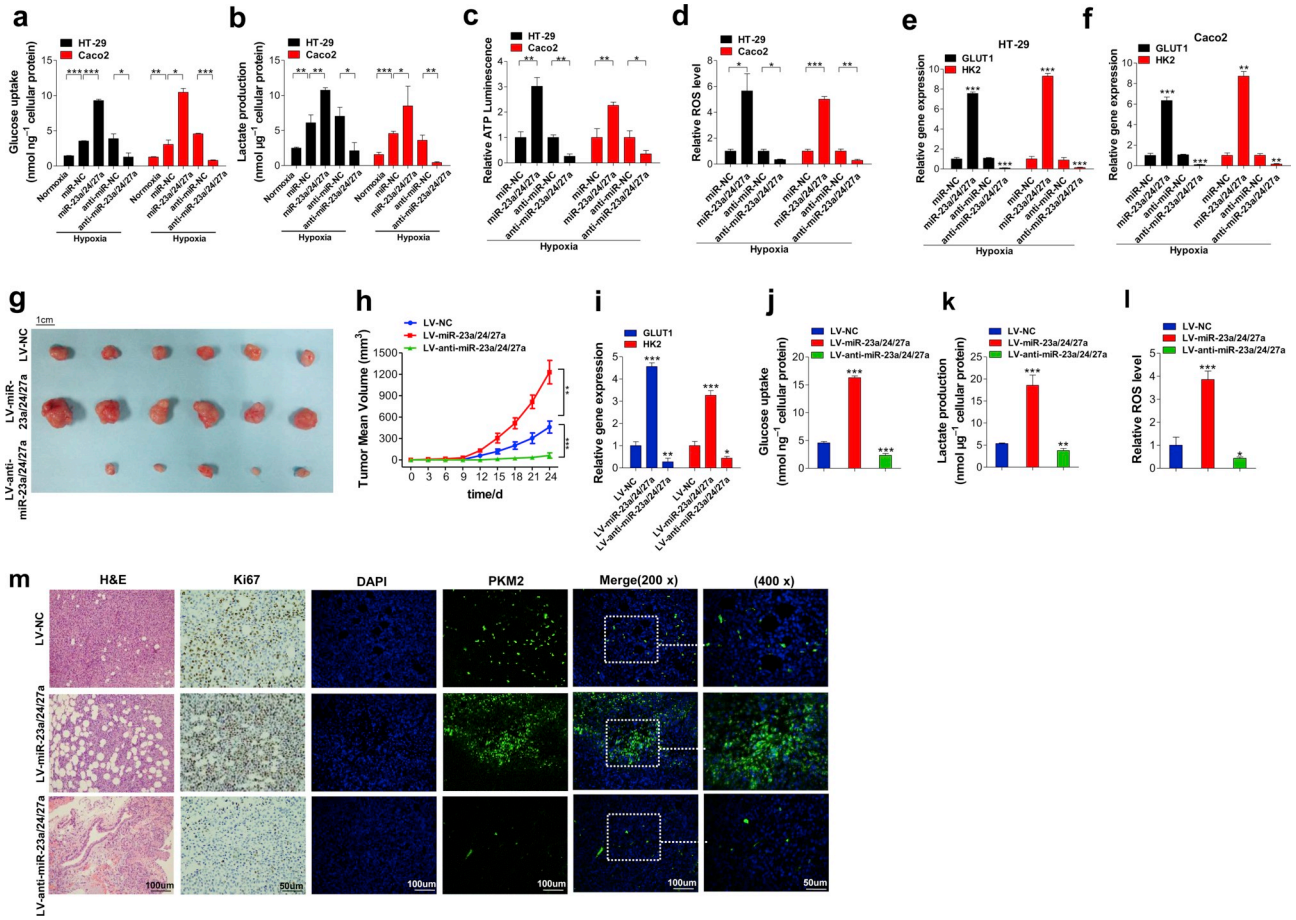

Fig. 3. The miR-23a ~ 27a ~ 24 cluster promotes glycolysis in CRC cells and tumors. HT-29 and Caco2 cells were transfected with miR-NC, miR-23a/27a/24 mimics (a combination of the miR-23a mimic, miR-24 mimic and miR-27a mimic), anti-miR-NC and anti-miR-23a/27a/24 (a combination of the anti-miR-23a inhibitor, anti-miR-24 inhibitor and anti-miR-27a inhibitor) under hypoxia, normoxic cells served as controls. A series of metabolic parameters was measured: **(a)** glucose uptake, **(b)** lactate production, **(c)** cellular ATP levels and **(d)** ROS levels. **(e, f)** qRT-PCR analysis showing the relative expression of GLUT1 and HK2 in HT-29 and Caco2 cells with different transfections under hypoxia. Then HT-29 cells were infected with control lentiviral vector, miR-23a/27a/24 lentiviral vectors or anti-miR-23a/27a/24 lentiviral vectors. Mice were divided into three groups according to the implanted HT-29 cell type: control cells (LV-NC), miR-23a/27a/24-overexpressing cells (LV-miR-23a/27a/24) and anti-miR-23a/27a/24 cells (LV-anti-miR-23a/27a/24), 6 mice/group. **(g)** Images of the tumors. **(h)** The time course of the tumor volume. **(i)** qRT-PCR analysis showing the relative expression of GLUT1 and HK2 in the tumors. The tumors were minced, ground, digested, and filtered to obtain individual cells, then cultured and metabolic parameters was measured: **(j)** glucose uptake, **(k)** lactate production, and **(l)** ROS levels. **(m)** H&E, Ki67 and PKM2 immunofluorescence staining in tumors from three groups of mice. Green indicates PKM2; blue indicates the nuclei. Data are shown as the mean ± S.E. of three separate experiments. *P < 0.05, **P < 0.01, ***P < 0.001. (For interpretation of the references to color in this figure legend, the reader is referred to the Web version of this article.)

mice. The xenograft experiments showed that the growth and sizes of tumors that stably overexpressed miR-23a/27a/24 (LV-miR-23a/24/27a) were significantly enhanced compared with those in control (LV-NC) group. However, when miR-23a/27a/24 was knocked down, tumor growth was clearly restrained (Fig. 3g and h). After 24 days, we euthanized the mice and harvested tumors for further analyses. qRT-PCR analysis showed that the GLUT1 and HK2 levels in miR-23a/27a/24 tumors were significantly increased relative to control group, but anti-miR-23a/27a/24 effectively reduced GLUT1 and HK2 expression (Fig. 3i). The tumors were minced, ground, digested, and filtered to obtain individual cells. Then the cells were cultured and metabolic parameters were measured. Our results showed that the glucose uptake, lactate production and ROS levels of miR-23a/27a/24-overexpressing tumors were much higher than control group, whereas these parameters were significantly reduced in anti-miR-23a/27a/24 group (Fig. 3j-l, Supplementary Fig. 4B). Additionally, hematoxylin and eosin (H&E) and immunohistochemical staining showed more mitotic and Ki67-positive cells in miR-23a/27a/24 tumors than control group, whereas the tumors in anti-miR-23a/27a/24 group showed lower mitosis and Ki67 levels than control group (Fig. 3m, Supplementary Fig. 5A). Because the glycolytic enzyme pyruvate kinase M2 (PKM2) is the major pyruvate kinase isozyme in tumors and is a pivotal player in glycolysis [40,41], we measured the PKM2 levels. Immunofluorescence staining showed that PKM2 expression was significantly increased in tumors from miR-23a/27a/24 group compared with control group, however, the PKM2 level significantly reduced in tumors from anti-miR-23a/27a/24 group compared with those in control group (Fig. 3m, Supplementary Fig. 5B). Taken together, these results indicate that miR-23a ~ 27a ~ 24 cluster facilitates glycolytic metabolism in CRC cells and tumors and further promotes tumor growth.

3.5. *The miR-23a ~ 27a ~ 24 cluster promotes the glycolytic switch via regulating relevant gene networks*

To characterize the molecular mechanisms by which miR-23a ~ 27a ~ 24 cluster regulates glucose metabolism, HT-29 cells were transfected with NC, anti-miR-23a, anti-miR-24 and anti-miR-27a and cultured under hypoxia for 48 h. The non-transfected HT-29 cells cultured under normoxia were used as control. Immunoblot analysis confirmed that inhibition of the three miRNAs effectively weakened the

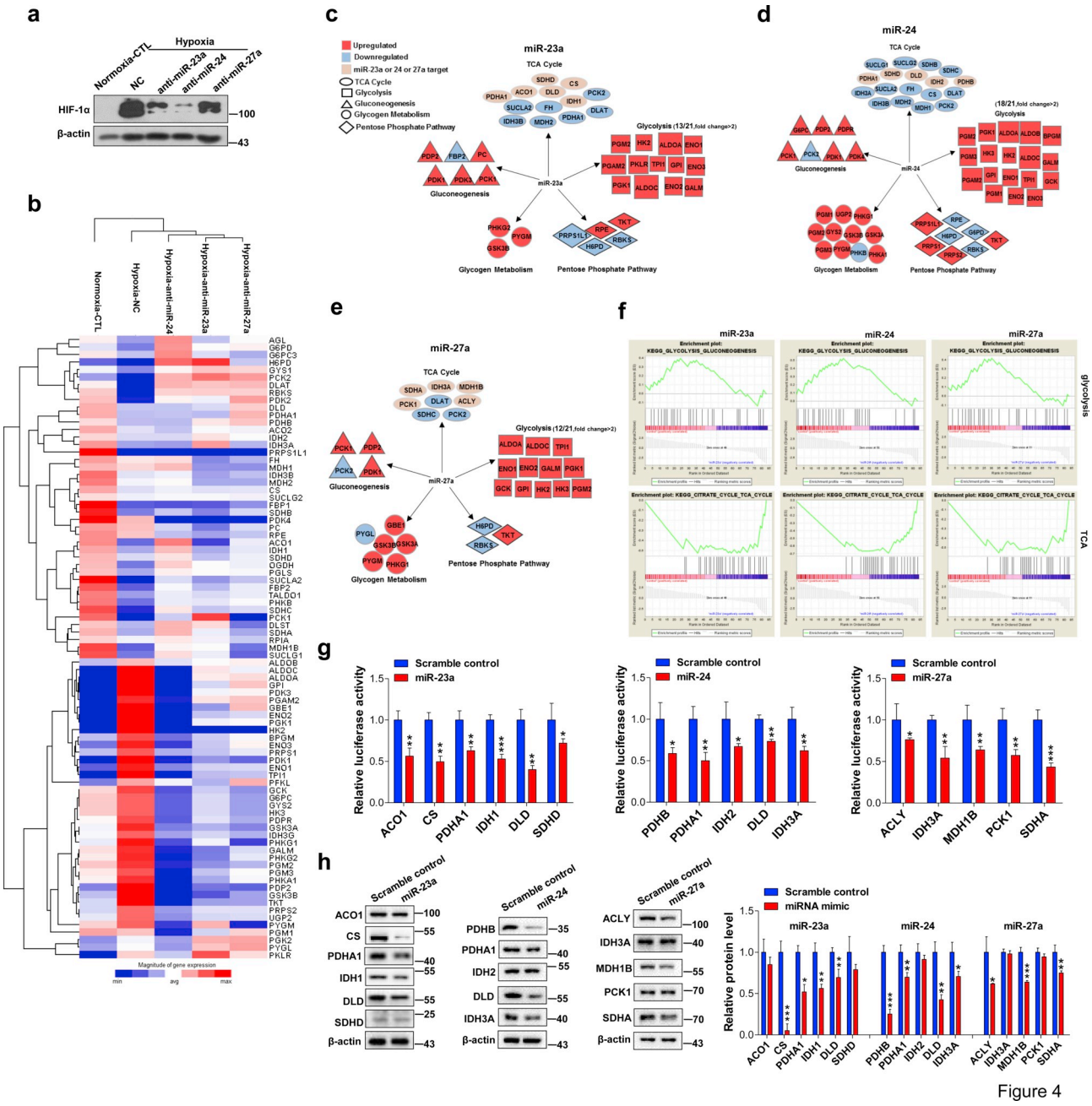

Figure 4

Fig. 4. MiR-23a ~ 27a ~ 24 cluster collectively regulate glycolytic switch via collaborative regulating relevant gene networks. (a) HT-29 cells were transfected with NC, anti-miR-23a, anti-miR-24 and anti-miR-27a and cultured under hypoxia for 48 h. Non-transfected HT-29 cells cultured for 48 h under normoxia were used as control. Representative western blotting analyses of HIF-1α were shown. **(b)** A human glucose metabolism PCR array was used to quantify 84 glucose metabolism-associated genes in HT-29 cells transfected with miR-NC, anti-miR-23a, anti-miR-24 and anti-miR-27a under hypoxia or normoxia. **(c–e)** Metabolism-associated gene networks that are regulated by miR-23a, miR-24 and miR-27a. Red node, upregulated genes; blue node, downregulated genes. **(f)** GSEA of miR-23a, miR-24 and miR-27a. The enrichment scores (shown in the upper curve) were calculated along the ranked genes. (In the bottom histogram, the upregulated to downregulated genes are shown from left to right). The vertical lines in the middle indicate the locations of the members in the gene set. **(g)** Dual luciferase activity in 293T cells that were transfected with firefly luciferase reporters containing the 3′UTRs of target genes and miRNAs. **(h)** HT-29 cells were transfected with scramble RNA, miR-23a mimic, miR-24 mimic and miR-27a mimic, respectively. The target gene expression levels were examined by immunoblotting. β-actin was served as internal control. Data are shown as the mean ± S.E. of three separate experiments. *P < 0.05, **P < 0.01, ***P < 0.001. (For interpretation of the references to color in this figure legend, the reader is referred to the Web version of this article.)

stimulatory effect of hypoxia on HIF-1α, and inhibition of miR-24 showed the most obvious recovery effect (Fig. 4a, Supplementary Fig. 6). Then a human glucose metabolism array was used to assess the expression alterations of genes (84 in total) associated with glucose metabolism. Supplementary Table 3 shows the changes of mRNA levels of genes involved in glucose metabolism that were measured using an RT^2 Profiler PCR Array [10,21]. The expression levels of glycolysis pathway-related genes (e.g., HK2, ALDOA, ALDOC, ENO1, ENO2, ENO3, GPI and PGAM2) were increased in hypoxia-treated cells (hypoxia-miR-NC) compared with normoxia control cells (CTL), whereas the TCA cycle-related genes (e.g., CS, DLD, PDHA1, ACO1, PDHB, SDHA and SDHB) were downregulated (Fig. 4b). Additionally, inhibition of miR-23a, miR-24 and miR-27a under hypoxia weakened the stimulatory effect of hypoxia on glycolysis-related genes and the

inhibitory effect on TCA cycle-related genes. Among these, miR-24 inhibition showed the most obvious effect (Fig. 4b). Then we further analyzed the reciprocal effect between the three miRNAs and investigated the regulatory subnetworks of them on glucose metabolism. Interestingly, miR-23a, miR-24 and miR-27a promoted the expression of glycolysis pathway-related genes and reduced the expression of TCA cycle metabolic genes. Among the genes in glycolysis pathway, 13/21 genes (61.9%) were upregulated by ~2-fold by miR-23a. Likewise, for the glycolysis-related genes regulated by miR-24 and miR-27a, 18/21 (85.7%) and 12/21 (57.1%) genes were increased by ~2-fold, respectively. However, most of the TCA cycle genes showed a general tendency toward decreased gene expression (Fig. 4c–e). Based on the metabolic gene expression profile from the PCR array results, we further examined the regulatory effects of three miRNAs on glycolysis and TCA pathways with a gene set enrichment analysis (GSEA) [38,42]. The results demonstrated that miR-23a, miR-24 and miR-27a promoted the expression of glycolysis-related genes, whereas TCA-related genes were downregulated by the miR-23a/27a/24 cluster (Fig. 4f). Taken together, these data suggest an active role for miR-23a~27a~24 cluster in regulating the cellular glucose metabolic pathways corporately.

To explore the underneath mechanism, we predicted whether the TCA-related genes were targets of miR-23a~27a~24 cluster. The predicted interactions between miRNAs and 3′-UTR regions of target genes are illustrated in Supplementary Fig. 7. Luciferase assays were further used to verify the regulation relationship. We identified several previously undefined targets of miR-23a~27a~24 cluster, including TCA cycle enzymes ACO1, CS, PDHA1, IDH1, DLD and SDHD, which were targeted by miR-23a, PDHB, PDHA1, IDH2, DLD and IDH3A, which were targeted by miR-24, and ACLY, IDH3A, MDH1B, PCK1 and SDHA, which were targeted by miR-27a (Fig. 4g). Then we further validate the interactions between miRNAs and target genes by western blot, the results demonstrated that miR-23a directly inhibited the expression of CS, PDHA1, IDH1 and DLD, miR-23a directly inhibited PDHB, PDHA1, DLD and IDH3A expression, miR-27a directly inhibited the expression of ACLY, MDH1B and SDHA (Fig. 4h). In summary, these data highlight the cooperative effects of miR-23a~27a~24 cluster on regulating glucose metabolism.

3.6. MiR-24 promotes HIF-1α expression by targeting VHL and forming a double-negative feedback loop

We next explored why miR-24 showed the strongest regulatory effect. HIF-1α is a key regulator of the transcriptional response to hypoxia and is strongly implicated in glycolysis, while VHL mediates the ubiquitination of HIF-1α and leads to rapid HIF-1α proteasomal degradation under normoxic conditions [14,16]. VHL/HIF-1α pathway plays vital roles in CRC progression [43]. Interestingly, we identified VHL as a direct target of miR-24 using luciferase assays and immunoblots (Fig. 5a, Supplementary Figs. 8A–D). Thus, HIF-1α may be recruited to miR-23a~27a~24 promoter to induce the cluster expression. Of them, miR-24 target and negatively regulate VHL expression, resulting in further increased expression of HIF-1α, which implies that HIF-1α, miR-24 and VHL do not work alone but instead form a double-negative feedback loop. To examine whether miR-24 promoted HIF-1α expression by inhibiting VHL, we transfected HT-29 and Caco2 cells with miR-NC, miR-24 mimic, VHL-expressing plasmid, miR-24 mimic plus VHL-expressing plasmid, anti-miR-24 inhibitor, VHL siRNA and anti-miR-24 inhibitor plus VHL siRNA under normoxia (Supplementary Fig. 8E). As shown in Fig. 5b and c and Supplementary Figs. 8F–I, VHL-expressing plasmid increased the VHL protein level, whereas co-transfection with miR-24 mimic attenuated the overexpression effect of VHL-expressing plasmid in CRC cells. In the presence of oxygen, HIF-1α is rapidly degraded and difficult to detect in cell lysates, whereas HIF-1α is detectable in isolated nuclei [16,43]. Then we isolated and detected nuclei from cells and showed that miR-24 overexpression led to an elevated HIF-1α level, whereas co-transfected VHL-expressing plasmid attenuated the stimulatory impact of miR-24 on HIF-1α. VHL knockdown by siRNA effectively attenuated the stimulatory effect of anti-miR-24 on VHL, whereas restored the inhibitory effect of anti-miR-24 on HIF-1α in nuclei. Under hypoxia, inhibition of miR-24 effectively attenuated the stimulatory effect of hypoxia on HIF-1α (Fig. 5d, Supplementary Fig. 8J). Whereas miR-24 overexpression effectively restored the inhibitory effect of HIF-1α siRNA on HIF-1α in HT-29 cells (Fig. 5e). Moreover, in HT-29 and Caco2 cells, miR-24 overexpression led to a significant increase of miR-23a and miR-27a, while miR-24 inhibition led to decrease of miR-23a and miR-27a (Supplementary Figs. 9A and B). Together, these results suggest that HIF-1α-induced miR-24 promotes HIF-1α expression by inhibiting VHL, which forms a double-negative (overall positive) feedback loop.

We further examined the correlation between HIF-1α, miR-24 and VHL in 36 pairs of clinical samples. Consistent with the upregulated expression of miR-24 (Fig. 1d), HIF-1α was also strongly expressed in CRC tumors (Fig. 5f), while VHL protein levels were consistently downregulated (Fig. 5f). HIF-1α/VHL ratio was consistently upregulated in CRC tumors (Fig. 5g). Importantly, Spearman correlation analysis revealed that there was a significantly positive correlation between miR-24 levels and HIF-1α/VHL ratio levels ($R = 0.875$, $P < 0.0001$) (Fig. 5h). Collectively, these results support the idea that HIF-1α-induced miR-24 positively promotes the expression of HIF-1α by inhibiting VHL, thereby forming a double-negative feedback loop.

3.7. HIF-1α/miR-24/VHL loop promotes CRC glycolysis in vitro and in vivo

To further examine the effects of HIF-1α/miR-24/VHL feedback loop on glycolysis, we transfected HT-29 cells with NC, miR-24 mimic and miR-24 mimic plus VHL-expressing plasmid under hypoxia and found that co-transfection of VHL-expressing plasmid attenuated the overexpression effect of miR-24 mimic on HIF-1α (Supplementary Fig. 10A). Moreover, qRT-PCR analysis showed that co-transfection of VHL-expressing plasmid weakened the stimulatory effect of miR-24 on HK2 and GLUT1 expression (Fig. 6a). Measurements of metabolic parameters revealed that the glucose uptake, lactate production, and cellular ATP and ROS levels were increased in cells transfected with miR-24 mimic, whereas co-transfection of VHL-expressing plasmid attenuated the stimulatory effect of miR-24 on these metabolic parameters (Fig. 6b–e, Supplementary Fig. 10B). Furthermore, VHL silencing decreased VHL expression (Supplementary Fig. 11 A-C) and increased these metabolic parameters (Supplementary Fig. 11 D-G).

To further evaluate the role of HIF-1α/miR-24/VHL on tumor growth and metabolism *in vivo*, a mouse tumor model was developed. HT-29 cells (1×10^6 cells per 0.1 ml) infected with miR-24-expressing lentivirus or a VHL overexpression plasmid were implanted subcutaneously into 6-week-old nude mice, respectively. The xenograft experiments revealed enhanced tumor sizes and masses for CRC cells that stably overexpressed miR-24 compared with those in control group. Cells expressing VHL-expressing plasmid formed tumors less easily, and co-overexpression of miR-24 and VHL attenuated the promoting effect of miR-24 on tumor growth (Fig. 6f–h). Lysates from tumor tissues revealed that tumors from LV-miR-24 group exhibited higher HIF-1α, PKM2 levels and lower VHL expression than control group and tumors from VHL group exhibited reduced PKM2, HIF-1α levels and increased VHL levels (Fig. 6i, Supplementary Figs. 12A–D). Moreover, qRT-PCR analysis showed that the GLUT1, HK2 and miR-24 levels in miR-24-overexpressing group were increased compared with those in control group, whereas tumors from VHL-overexpressing group exhibited strongly reduced levels of miR-24, GLUT1, and HK2 (Fig. 6j, Supplementary Fig. 12). Tumors from LV-miR-24 group showed higher mitosis, Ki67 and PKM2 levels and lower VHL level than control group, whereas the tumors in LV-miR-24 + VHL group showed lower mitosis, Ki67 and PKM2 levels and higher VHL levels than LV-miR-24 group (Supplementary Fig. 12E). These results are consistent with the *in vitro* data and validate the biological role of the HIF-1α/miR-24/VHL loop in

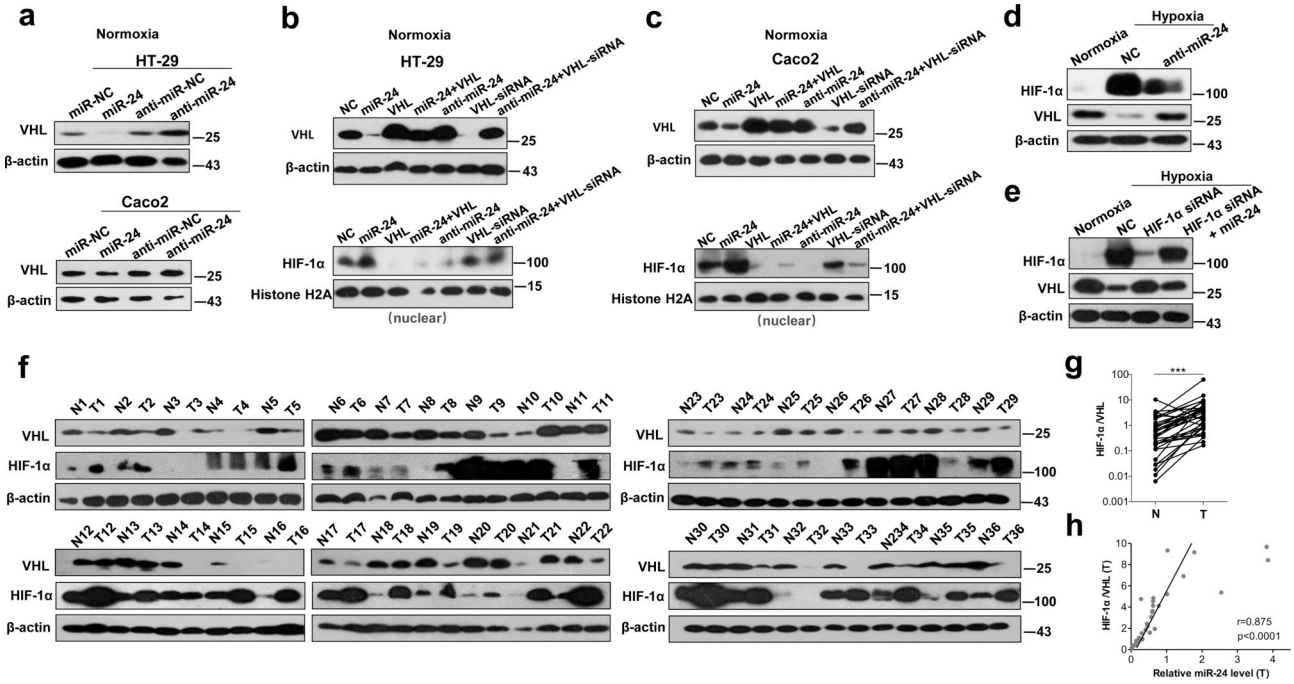

Fig. 5. miR-24 promotes the expression of HIF-1α by targeting VHL. (a) HT-29 and Caco2 cells were transfected with miR-NC, miR-24 mimic, anti-miR-NC and anti-miR-24 under normoxia. VHL expression levels were examined by immunoblotting. β-actin was served as internal control. **(b, c)** HT-29 and Caco2 cells that were transfected with NC, the miR-24 mimic, the VHL expression vector (VHL), the miR-24 mimic plus VHL expression vector, anti-miR-24, VHL siRNA and anti-miR-24 plus VHL siRNA were cultured under normoxia. The protein levels of HIF-1α in nuclear extracts (Histone H2A was served as internal control) and VHL in total cellular extracts (β-actin was served as internal control) are shown. **(d)** HT-29 cells transfected with NC and anti-miR-24 under hypoxia and compared to cells under normoxia. The total cellular protein levels for HIF-1α and VHL were examined. **(e)** HT-29 cells were transfected with NC, HIF-1α siRNA, HIF-1α siRNA plus miR-24 mimic under hypoxia, the cells under normoxia were used as control. The total cellular protein levels for HIF-1α and VHL were examined. β-actin was served as internal control. **(f)** The protein levels of VHL and HIF-1α were determined by immunoblotting of 36 pairs of clinical samples. β-actin was used as the internal control. **(g)** Quantitative analyses of the ratios of HIF-1α/VHL protein levels in tumor tissues (T) and normal adjacent tissues (N). n = 36 in each group. **(h)** Pearson's correlation scatter plot of the fold changes of miR-24 and HIF-1α/VHL ratios in CRC tissues. Data are shown as the mean ± S.E. of three separate experiments. **P < 0.01; ***P < 0.001.

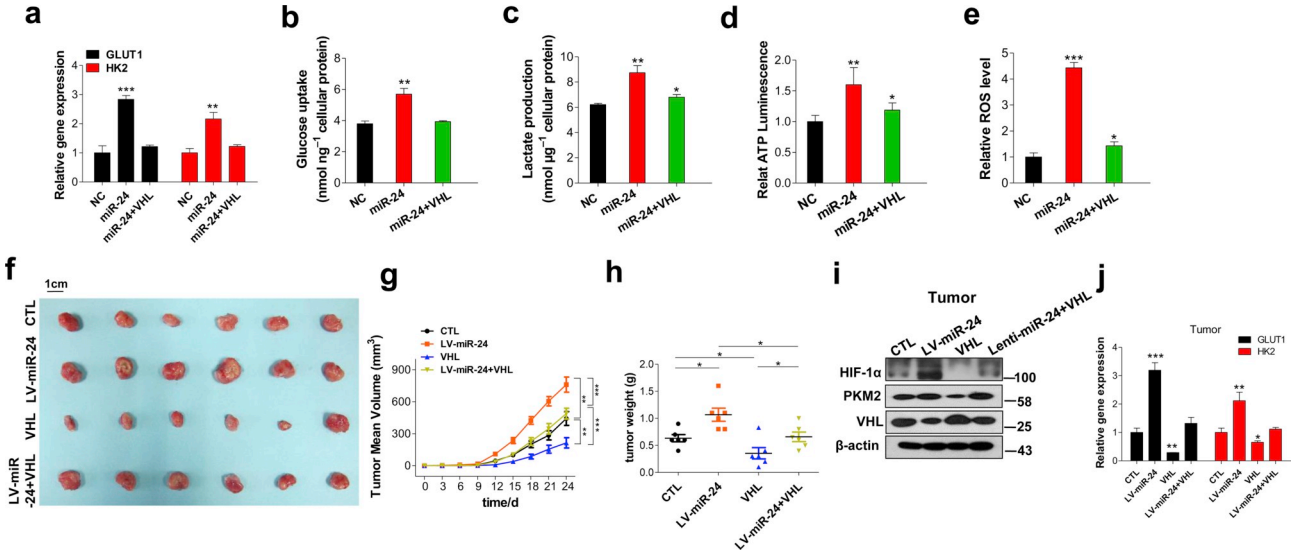

Fig. 6. The HIF-1α/miR-24/VHL loop plays an important role in promoting glycolysis *in vitro* and *in vivo*. HT-29 cells were transfected with NC, miR-24 mimic, or miR-24 mimic plus VHL expression vector under hypoxia for 48 h **(a)** qRT-PCR analysis showing the relative expression of GLUT1 and HK2, **(b)** glucose uptake, **(c)** lactate production, **(d)** cellular ATP levels and **(e)** ROS levels. Then HT-29 cells were infected with control lentiviral vector, miR-24 lentiviral vectors, VHL-overexpressing plasmids and miR-24 lentiviral vector plus VHL-overexpressing plasmid. Mice were divided into four groups according to the implanted HT-29 cell type: control cells (CTL), miR-24-overexpressing cells (LV-miR-24), VHL-overexpressing cells (VHL), and VHL plus miR-24-overexpressing cells (LV-miR-24 + VHL). **(f)** Representative images of the tumors. **(g)** The time course of the tumor volume. **(h)** The quantitative analysis of the tumor weights. **(i)** Western blot analyses of the HIF-1α, VHL, and PKM2 proteins in tumors from four groups. **(j)** qRT-PCR analysis showing the relative expression of GLUT1 and HK2 in tumors. Data are shown as the mean ± S.E. of three separate experiments. *P < 0.05, **P < 0.01, ***P < 0.001.

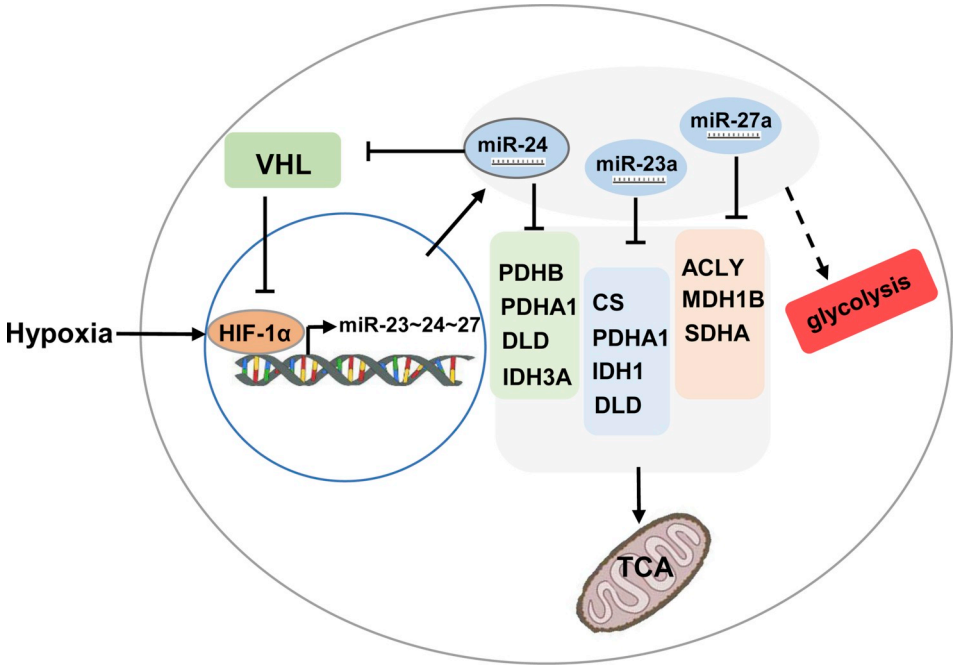

Fig. 7. Model of the miR-23a ~ 27a ~ 24 cluster as a key regulatory node that links hypoxia to promoting glycolysis in CRC.

modulating CRC metabolism and progression.

4. Discussion

As an inherent feature of solid tumors, hypoxia contributes to the reprogramming of cancer metabolism from oxidative phosphorylation to glycolysis [1,2,44]. However, the critical determinants of this switch, particularly the initiating and limiting factors that regulate entry into the reprogramming process, are poorly understood. MiRNAs have emerged as major regulators of various physiological and pathological cellular processes, including hypoxia and metabolic reprogramming [9]. Individual miRNAs can either restrict or enhance cancer metabolism reprogramming. For example, hypoxia-suppressed miR-199a and miR-125a play important roles in limiting glycolysis in HCC cells [10,11], whereas miR-448 promotes glycolytic metabolism in gastric cancer [45]. However, a key feature of a single miRNA action is its modest quantitative effect on an individual direct mRNA target.

One remarkable aspect of miRNAs is that they are often organized as clusters (within 3 kb) in the genome [46]. Generally, miRNA clusters are transcribed coordinately as polycistronic units that are processed to produce individual miRNAs, resulting in co-expression of the miRNAs [12,13]. Importantly, miRNA clusters function by repressing multiple target genes coordinately [33,47], which is a property that we exploited to uncover the regulatory networks that govern cancer metabolism. This study showed that the miR-23a ~ 27a ~ 24 cluster consists of the most upregulated of hypoxia-induced miRNAs in CRC. Additionally, miR-23a ~ 27a ~ 24 cluster collectively regulates glucose metabolism and shifts the metabolic balance toward glycolysis. This type of regulation is important in tumorigenesis. Coordinate regulation by the cluster may provoke a rapid switch in metabolic signaling network of cancer cells. Generally, the effect of an individual miRNA is relatively weak, however, when several miRNAs act in combination, the effect can be efficient and potent [12,47–49].

Each miRNA targets hundreds of mRNAs, and a collaborative inhibition of numerous direct targets in gene networks can have substantial biological consequences [49]. This property can be used to connect miRNAs to previously described pathways and to uncover regulators of cell processes. The current paradigm for miRNA function posits that miRNAs mediate their effects by affecting the expression of multiple direct targets in common biological networks [33,42]. Therefore, we predicted all the target genes of miR-23a, miR-27a and miR-24, performed GO and KEGG analyses and showed that most of target genes of the cluster were enriched for regulation of metabolism-related processes and signaling pathways in CRC. Furthermore, we combined bioinformatics and experimental approaches and found that miR-23a ~ 27a ~ 24 cluster directly targeted genes in networks of highly interconnected nodes of TCA cycle, which is consistent with the possibility that dozens of targets contribute to cancer metabolic reprogramming effects of this miRNA cluster. Our results provide a novel and reliable way to explore miRNA functions in tumor metabolism and suggest that miR-23a ~ 27a ~ 24 cluster is not only a “participator” but also a “decider” in the glucose metabolism reprogramming.

HIF-1α-mediated transcriptional regulation plays an important role in hypoxia [1], HIF-1α controls genes that are critical to cancer metabolism [2]. In this study, we found that HIF-1α can directly bind to the promoter of miR-23a ~ 27a ~ 24 cluster to induce miRNA expression. Among the three miRNAs, miR-24 can, in turn, promote HIF-1α expression by inhibiting VHL. VHL is a key regulator of HIF-1α stability that functions by mediating HIF-1α ubiquitination and degradation [14,50]. Some reports have described that miR-24 increases HIF-1α expression by targeting FIH1, an asparaginyl β-hydroxylase that promotes transcriptional repression of HIF-1 [51]. Our results demonstrate that HIF-1α-induced miR-24 upregulation is crucial for the glycolysis-promoting effect of hypoxia via VHL targeting, which weakens the inhibitory effect of VHL on HIF-1α and consequently forms a double-negative feedback loop. Importantly, double-negative feedback is equivalent to positive feedback and amplifies the signal and reinforce the cell decision-making process during cellular growth [52,53]. In this case, the double-negative feedback promotes the cancer cell transition into the “high HIF-1α/miR-24 and low VHL” state, which is more favorable for cell survival.

Taken together, we found that miR-23a, miR-24 and miR-27a were induced by HIF-1α under hypoxia and the miRNA cluster regulates cancer metabolism reprogramming in CRC coordinately. As shown in Fig. 7, a screen of candidate targets revealed the target networks, which connected the predicted miR-23a ~ 27a ~ 24 targets to TCA cycle. Among these, a double-negative feedback loop that comprised of miR-24, VHL and HIF-1α are formed, suggesting that miR-24 play an

important role in regulating HIF-1α expression and in turn regulating the expression of the whole miRNA cluster. Thus, identification of functionally relevant miRNAs and vulnerable nodes in the miRNA target networks may provide new information and hypotheses regarding the regulation of cancer metabolism.

Conflicts of interest

The authors declare that they have no competing interests.

Acknowledgements

This work was supported by grants from the National Natural Science Foundation of China (No. 31670917), the Natural Science Foundation of Jiangsu Province (BK20170076), the Six talent peaks project of Jiangsu Province (YY-012), the Fundamental Research Funds for the Central Universities (020814380039, 020814380082) and Nanjing University Innovation and Creative Program for PHD candidate (No. 2016025).

Appendix A. Supplementary data

Supplementary data to this article can be found online at https://doi.org/10.1016/j.canlet.2018.10.025.

References

[1] W.R. Wilson, M.P. Hay, Targeting hypoxia in cancer therapy, Nat. Rev. Canc. 11 (2011) 393–410.
[2] A.J. Majmundar, W.H.J. Wong, M.C. Simon, Hypoxia-inducible factors and the response to hypoxic stress, Mol. Cell. 40 (2010) 294–309.
[3] M.G. Vander Heiden, L.C. Cantley, C.B. Thompson, Understanding the Warburg effect: the metabolic requirements of cell proliferation, Science (New York, N.Y.) 324 (2009) 1029–1033.
[4] D.A. Tennant, R.V. Duran, E. Gottlieb, Targeting metabolic transformation for cancer therapy, Nat. Rev. Canc. 10 (2010) 267–277.
[5] N.H. Kim, Y.H. Cha, J. Lee, S.-H. Lee, J.H. Yang, J.S. Yun, E.S. Cho, X. Zhang, M. Nam, N. Kim, Y.-S. Yuk, S.Y. Cha, Y. Lee, J.K. Ryu, S. Park, J.-H. Cheong, S.W. Kang, S.-Y. Kim, G.-S. Hwang, J.I. Yook, H.S. Kim, Snail reprograms glucose metabolism by repressing phosphofructokinase PFKP allowing cancer cell survival under metabolic stress, Nat. Commun. 8 (2017).
[6] J.T. Leith, G. Padfield, L. Faulkner, S. Michelson, HYPOXIC FRACTIONS IN XENOGRAFTED HUMAN COLON TUMORS, Cancer Res. 51 (1991) 5139–5143.
[7] R.A. Gatenby, R.J. Gillies, Why do cancers have high aerobic glycolysis? Nat. Rev. Canc. 4 (2004) 891–899.
[8] D.P. Bartel, MicroRNAs: genomics, biogenesis, mechanism, and function, Cell 116 (2004) 281–297.
[9] W.P. Kloosterman, R.H.A. Plasterk, The diverse functions of MicroRNAs in animal development and disease, Dev. Cell 11 (2006) 441–450.
[10] F. Jin, Y. Wang, Y. Zhu, S. Li, Y. Liu, C. Chen, X. Wang, K. Zen, L. Li, The miR-125a/HK2 axis regulates cancer cell energy metabolism reprogramming in hepatocellular carcinoma, Sci. Rep. 7 (2017).
[11] L.-F. Zhang, J.-T. Lou, M.-H. Lu, C. Gao, S. Zhao, B. Li, S. Liang, Y. Li, D. Li, M.-F. Liu, Suppression of miR-199a maturation by HuR is crucial for hypoxia-induced glycolytic switch in hepatocellular carcinoma, EMBO J. 34 (2015) 2671–2685.
[12] Y. Wang, H. Liang, G. Zhou, X. Hu, Z. Liu, F. Jin, M. Yu, J. Sang, Y. Zhou, Z. Fu, C.-Y. Zhang, W. Zhang, K. Zen, X. Chen, HIC1 and miR-23 similar to 27 similar to 24 clusters form a double-negative feedback loop in breast cancer, Cell Death Differ. 24 (2017) 421–432.
[13] Y. Lee, K. Jeon, J.T. Lee, S. Kim, V.N. Kim, MicroRNA maturation: stepwise processing and subcellular localization, EMBO J. 21 (2002) 4663–4670.
[14] P.H. Maxwell, M.S. Wiesener, G.W. Chang, S.C. Clifford, E.C. Vaux, M.E. Cockman, C.C. Wykoff, C.W. Pugh, E.R. Maher, P.J. Ratcliffe, The tumour suppressor protein VHL targets hypoxia-inducible factors for oxygen-dependent proteolysis, Nature 399 (1999) 271–275.
[15] L.E. Huang, J. Gu, M. Schau, H.F. Bunn, Regulation of hypoxia-inducible factor 1 alpha is mediated by an O-2-dependent degradation domain via the ubiquitin-proteasome pathway, Proc. Natl. Acad. Sci. U.S.A. 95 (1998) 7987–7992.
[16] W.G. Kaelin Jr., P.J. Ratcliffe, Oxygen sensing by metazoans: the central role of the HIF hydroxylase pathway, Mol. Cell. 30 (2008) 393–402.
[17] G.L. Semenza, HIF-1: upstream and downstream of cancer metabolism, Curr. Opin. Genet. Dev. 20 (2010) 51–56.
[18] G.P. Nagaraju, P.V. Bramhachari, G. Raghu, B.F. El-Rayes, Hypoxia inducible factor-1 alpha: its role in colorectal carcinogenesis and metastasis, Cancer Lett. 366 (2015) 11–18.
[19] J. Ma, H. Wang, R. Liu, L. Jin, Q. Tang, X. Wang, A. Jiang, Y. Hu, Z. Li, L. Zhu, R. Li, M. Li, X. Li, The miRNA transcriptome directly reflects the physiological and biochemical differences between red, white, and intermediate muscle fiber types, Int. J. Mol. Sci. 16 (2015) 9635–9653.
[20] F. Jin, Y. Wang, M. Li, Y. Zhu, H. Liang, C. Wang, F. Wang, C.-Y. Zhang, K. Zen, L. Li, MiR-26 enhances chemosensitivity and promotes apoptosis of hepatocellular carcinoma cells through inhibiting autophagy, Cell Death Dis. 8 (2017).
[21] C. Broder, P. Arnold, S. Vadon-Le Goff, M.A. Konerding, K. Bahr, S. Muller, C.M. Overall, J.S. Bond, T. Koudelka, A. Tholey, D.J.S. Hulmes, C. Moali, C. Becker-Pauly, Metalloproteases meprin alpha and meprin beta are C- and N-procollagen proteinases important for collagen assembly and tensile strength, Proc. Natl. Acad. Sci. U.S.A. 110 (2013) 14219–14224.
[22] D. Wang, X. Sun, Y. Wei, H. Liang, M. Yuan, F. Jin, X. Chen, Y. Liu, C.-Y. Zhang, L. Li, K. Zen, Nuclear MiR-122 Directly Regulates the Biogenesis of Cell Survival OncomiR MiR-21 at the Posttranscriptional Level, Nucleic acids research, 2017.
[23] X. Ma, C. Li, L. Sun, D. Huang, T. Li, X. He, G. Wu, Z. Yang, X. Zhong, L. Song, P. Gao, H. Zhang, Lin28/let-7 axis regulates aerobic glycolysis and cancer progression via PDK1, Nat. Commun. 5 (2014).
[24] R. Requejo-Aguilar, I. Lopez-Fabuel, E. Fernandez, L.M. Martins, A. Almeida, J.P. Bolanos, PINK1 deficiency sustains cell proliferation by reprogramming glucose metabolism through HIF1, Nat. Commun. 5 (2014).
[25] Y. Chang, W. Yan, X. He, L. Zhang, C. Li, H. Huang, G. Nace, D.A. Geller, J. Lin, A. Tsung, miR-375 inhibits autophagy and reduces viability of hepatocellular carcinoma cells under hypoxic conditions, Gastroenterology 143 (2012) 177–U357.
[26] X.X. He, Y. Chang, F.Y. Meng, M.Y. Wang, Q.H. Xie, F. Tang, P.Y. Li, Y.H. Song, J.S. Lin, MicroRNA-375 targets AEG-1 in hepatocellular carcinoma and suppresses liver cancer cell growth in vitro and in vivo, Oncogene 31 (2012) 3357–3369.
[27] J.F. Wei, H.L. Li, S.H. Wang, T.P. Li, J.F. Fan, X.L. Liang, J. Li, Q. Han, L. Zhu, L.Y. Fan, R.C. Zhao, let-7 enhances osteogenesis and bone formation while repressing adipogenesis of human stromal/mesenchymal stem cells by regulating HMGA2, Stem Cell. Dev. 23 (2014) 1452–1463.
[28] L. Yu, W. Di, H. Gao, J.J. Balic, A. Tsykin, T.-S. Han, Y.D. Liu, C.L. Kennedy, J.K. Li, J.Q. Mao, P. Tan, M. Oshima, G.J. Goodall, B.J. Jenkins, Clinical utility of a STAT3-regulated miRNA-200 family signature with prognostic potential in early gastric cancer, Clin. Canc. Res. 24 (2018) 1459–1472.
[29] W. Luo, H. Hu, R. Chang, J. Zhong, M. Knabel, R. O'Meally, R.N. Cole, A. Pandey, G.L. Semenza, Pyruvate kinase M2 is a PHD3-stimulated coactivator for hypoxia-inducible factor 1, Cell 145 (2011) 732–744.
[30] A. Kaidi, D. Qualtrough, A.C. Williams, C. Paraskeva, Direct transcriptional up-regulation of cyclooxygenase-2 by hypoxia-inducible factor (HIF)-1 promotes colorectal tumor cell survival and enhances HIF-1 transcriptional activity during hypoxia, Cancer Res. 66 (2006) 6683–6691.
[31] J.Q. Wang, K.W. Hu, J.W. Guo, F.X. Cheng, J. Lv, W.H. Jiang, W.Q. Lu, J.S. Liu, X.F. Pang, M.Y. Liu, Suppression of KRas-mutant cancer through the combined inhibition of KRAS with PLK1 and ROCK, Nat. Commun. 7 (2016) 13.
[32] C.-J. Guo, Q. Pan, D.-G. Li, H. Sun, B.-W. Liu, miR-15b and miR-16 are implicated in activation of the rat hepatic stellate cell: an essential role for apoptosis, J. Hepatol. 50 (2009) 766–778.
[33] S. Izreig, B. Samborska, R.M. Johnson, A. Sergushichev, E.H. Ma, C. Lussier, E. Loginicheva, A.O. Donayo, M.C. Poffenberger, S.M. Sagan, E.E. Vincent, M.N. Artyomov, T.F. Duchaine, R.G. Jones, The mir-17 similar to 92 microRNA cluster is a global regulator of tumor metabolism, Cell Rep. 16 (2016) 1915–1928.
[34] C. Van Dang, Myc, metabolism, and cancer, Clin. Canc. Res. 22 (2016) 1.
[35] P. Gao, H. Zhang, R. Dinavahi, F. Li, Y. Xiang, V. Raman, Z.M. Bhujwalla, D.W. Felsher, L. Cheng, J. Pevsner, L.A. Lee, G.L. Semenza, C.V. Dang, HIF-dependent antitumorigenic effect of antioxidants in vivo, Cancer Cell 12 (2007) 230–238.
[36] R.J. DeBerardinis, Is cancer a disease of abnormal cellular metabolism? New angles on an old idea, Genet. Med. 10 (2008) 267–277.
[37] S.Y. Lunt, M.G. Vander Heiden, Aerobic glycolysis: meeting the metabolic requirements of cell proliferation, in: R. Schekman, L. Goldstein, R. Lehmann (Eds.) Annual Review of Cell and Developmental Biology, vol. 272011, pp. 441-464.
[38] L.W.S. Finley, A. Carracedo, J. Lee, A. Souza, A. Egia, J. Zhang, J. Teruya-Feldstein, P.I. Moreira, S.M. Cardoso, C.B. Clish, P.P. Pandolfi, M.C. Haigis, SIRT3 opposes reprogramming of cancer cell metabolism through HIF1 alpha destabilization, Cancer Cell 19 (2011) 416–428.
[39] J.L. O'Donnell, M.R. Joyce, A.M. Shannon, J. Harmey, J. Geraghty, D. Bouchier-Hayes, Oncological implications of hypoxia inducible factor-1 alpha (HIF-1 alpha) expression, Cancer Treat Rev. 32 (2006) 407–416.
[40] D. Anastasiou, G. Poulogiannis, J.M. Asara, M.B. Boxer, J.-k. Jiang, M. Shen, G. Bellinger, A.T. Sasaki, J.W. Locasale, D.S. Auld, C.J. Thomas, M.G. Vander Heiden, L.C. Cantley, Inhibition of pyruvate kinase M2 by reactive oxygen species contributes to cellular antioxidant responses, Science 334 (2011) 1278–1283.
[41] W. Luo, G.L. Semenza, Emerging roles of PKM2 in cell metabolism and cancer progression, Trends Endocrinol. Metabol. 23 (2012) 560–566.
[42] H.H. Pua, D.F. Steiner, S. Patel, J.R. Gonzalez, J.F. Ortiz-Carpena, R. Kageyama, N.-T. Chiou, A. Gallman, D. de Kouchkovsky, L.T. Jeker, M.T. McManus, D.J. Erle, K.M. Ansel, MicroRNAs 24 and 27 suppress allergic inflammation and target a network of regulators of T helper 2 cell-associated cytokine production, Immunity 44 (2016) 821–832.
[43] R.H. Giles, M.P. Lolkema, C.M. Snijckers, M. Belderbos, P. van der Groep, D.A. Mans, M. van Beest, M. van Noort, R. Goldschmeding, P.J. van Diest, H. Clevers, E.E. Voest, Interplay between VHL/HIF1 alpha and Wnt/beta-catenin pathways during colorectal tumorigenesis, Oncogene 25 (2006) 3065–3070.
[44] Y.J. Hao, Y. Samuels, Q.L. Li, D. Krokowski, B.J. Guan, C. Wang, Z.C. Jin, B.H. Dong, B. Cao, X.J. Feng, M. Xiang, C. Xu, S. Fink, N.J. Meropol, Y. Xu, R.A. Conlon, S. Markowitz, K.W. Kinzler, V.E. Velculescu, H. Brunengraber, J.E. Willis, T. LaFramboise, M. Hatzoglou, G.F. Zhang, B. Vogelstein, Z.H. Wang,

Oncogenic PIK3CA mutations reprogram glutamine metabolism in colorectal cancer, Nat. Commun. 7 (2016) 13.
[45] X. Hong, Y. Xu, X. Qiu, Y. Zhu, X. Feng, Z. Ding, S. Zhang, L. Zhong, Y. Zhuang, C. Su, X. Hong, J. Cai, MiR-448 promotes glycolytic metabolism of gastric cancer by downregulating KDM2B, Oncotarget 7 (2016) 22092–22102.
[46] S. Griffiths-Jones, H.K. Saini, S. van Dongen, A.J. Enright, miRBase: tools for microRNA genomics, Nucleic Acids Res. 36 (2008) D154–D158.
[47] S. Cho, C.J. Wu, T. Yasuda, L.O. Cruz, A.A. Khan, L.L. Lin, D.T. Nguyen, M. Miller, H.M. Lee, M.L. Kuo, D.H. Broide, K. Rajewsky, A.Y. Rudensky, L.F. Lu, miR-23 similar to 27 similar to 24 clusters control effector T cell differentiation and function, J. Exp. Med. 213 (2016) 235–249.
[48] M.S. Ebert, P.A. Sharp, Roles for MicroRNAs in conferring robustness to biological processes, Cell 149 (2012) 515–524.
[49] E.A. Miska, E. Alvarez-Saavedra, A.L. Abbott, N.C. Lau, A.B. Hellman, S.M. McGonagle, D.P. Bartel, V.R. Ambros, H.R. Horvitz, Most Caenorhabditis elegans microRNAs are individually not essential for development or viability, PLoS Genet. 3 (2007) 2395–2403.
[50] L. Gossage, T. Eisen, E.R. Maher, VHL, the story of a tumour suppressor gene, Nat. Rev. Canc. 15 (2015) 55–64.
[51] G. Roscigno, I. Puoti, I. Giordano, E. Donnarumma, V. Russo, A. Affinito, A. Adamo, C. Quintavalle, M. Todaro, M.d. Vivanco, G. Condorelli, MiR-24 induces chemotherapy resistance and hypoxic advantage in breast cancer, Oncotarget 8 (2017) 19507–19521.
[52] R.J. Johnston, S. Chang, J.F. Etchberger, C.O. Ortiz, O. Hobert, MicroRNAs acting in a double-negative feedback loop to control a neuronal cell fate decision, Proc. Natl. Acad. Sci. U.S.A. 102 (2005) 12449–12454.
[53] J.E. Ferrell, Self-perpetuating states in signal transduction: positive feedback, double-negative feedback and bistability, Curr. Opin. Cell Biol. 14 (2002) 140–148.